Pseudo-nitzschia bloom dynamics in the Gulf of Maine: 2012–2016

Suzanna Clark[a],[*], Katherine A. Hubbard[a],[b], Donald M. Anderson[a], Dennis J. McGillicuddy Jr.[a], David K. Ralston[a], David W. Townsend[c]

[a] *Woods Hole Oceanographic Institution, 86 Water St. MS 21 Woods Hole, MA, 02543, USA*
[b] *Florida Fish and Wildlife Conservation Commission-Fish and Wildlife Research Institute, 100 8th Ave SE, St. Petersburg, FL, 33701, USA*
[c] *University of Maine, Orono, ME 04469, USA*

ARTICLE INFO

ABSTRACT

The toxic diatom genus *Pseudo-nitzschia* is a growing presence in the Gulf of Maine (GOM), where regionally unprecedented levels of domoic acid (DA) in 2016 led to the first Amnesic Shellfish Poisoning closures in the region. However, factors driving GOM *Pseudo-nitzschia* dynamics, DA concentrations, and the 2016 event are unclear. Water samples were collected at the surface and at depth in offshore transects in summer 2012, 2014, and 2015, and fall 2016, and a weekly time series of surface water samples was collected in 2013. Temperature and salinity data were obtained from NERACOOS buoys and measurements during sample collection. Samples were processed for particulate DA (pDA), dissolved nutrients (nitrate, ammonium, silicic acid, and phosphate), and cellular abundance. Species composition was estimated via Automated Ribosomal Intergenic Spacer Analysis (ARISA), a semi-quantitative DNA finger-printing tool. *Pseudo-nitzschia* biogeography was consistent in the years 2012, 2014, and 2015, with greater *Pseudo-nitzschia* cell abundance and *P. plurisecta* dominance in low-salinity inshore samples, and lower *Pseudo-nitzschia* cell abundance and *P. delicatissima* and *P. seriata* dominance in high-salinity offshore samples. During the 2016 event, pDA concentrations were an order of magnitude higher than in previous years, and inshore-offshore contrasts in biogeography were weak, with *P. australis* present in every sample. Patterns in temporal and spatial variability confirm that pDA increases with the abundance and the cellular DA of *Pseudo-nitzschia* species, but was not correlated with any one environmental factor. The greater pDA in 2016 was caused by *P. australis* – the observation of which is unprecedented in the region – and may have been exacerbated by low residual silicic acid. The novel presence of *P. australis* may be due to local growth conditions, the introduction of a population with an anomalous water mass, or both factors. A definitive cause of the 2016 bloom remains unknown, and continued DA monitoring in the GOM is warranted.

1. Introduction

Domoic acid (DA) first came to international attention in 1987, when hundreds of people were poisoned and three people died after eating contaminated shellfish harvested on Prince Edward Island, Canada. The diatom *Nitzschia pungens* was identified as the culprit (Bates et al., 1989). Since then, *Nitzschia pungens* has been re-classified as *Pseudo-nitzschia multiseries*, 52 more *Pseudo-nitzschia* species have been identified, and 26 species have been shown to produce DA (Bates et al., 2018). *Pseudo-nitzschia* are typically lightly-silicified, cosmopolitan diatoms (Hasle, 2002) that have been found along the coastlines of every continent in the world (Trainer et al., 2012) and can tolerate a broad range of environmental conditions. Some species, such as *P. seriata*, can grow in temperatures from 4 °C (Hansen et al., 2011) to

15 °C (Fehling et al., 2004), and others, such as *P. multiseries*, can grow in salinities from 20 to 40 (Doucette et al., 2008; Thessen and Stoecker, 2008).

Toxic *Pseudo-nitzschia* blooms are traditionally associated with up-welling regions, but the genus has also been observed in oligotrophic gyres (Guannel et al., 2015), bays (Thorel et al., 2017) and shelf seas (Bresnan et al., 2015). Regime shifts in *Pseudo-nitzschia* absolute and relative abundance have been connected to changes in nutrient ratios (Lundholm et al., 2010; Parsons et al., 2002), remote physical forcing (Sekula-Wood et al., 2011), and temperature (Lundholm et al., 2010). In recent years, globally and regionally record-breaking blooms (in terms of DA concentrations and the extent of shellfishery closures) have occurred (McCabe et al., 2016; Bates et al., 2018)). In the Gulf of Maine (GOM), nine unique species of *Pseudo-nitzschia* had been identified as of
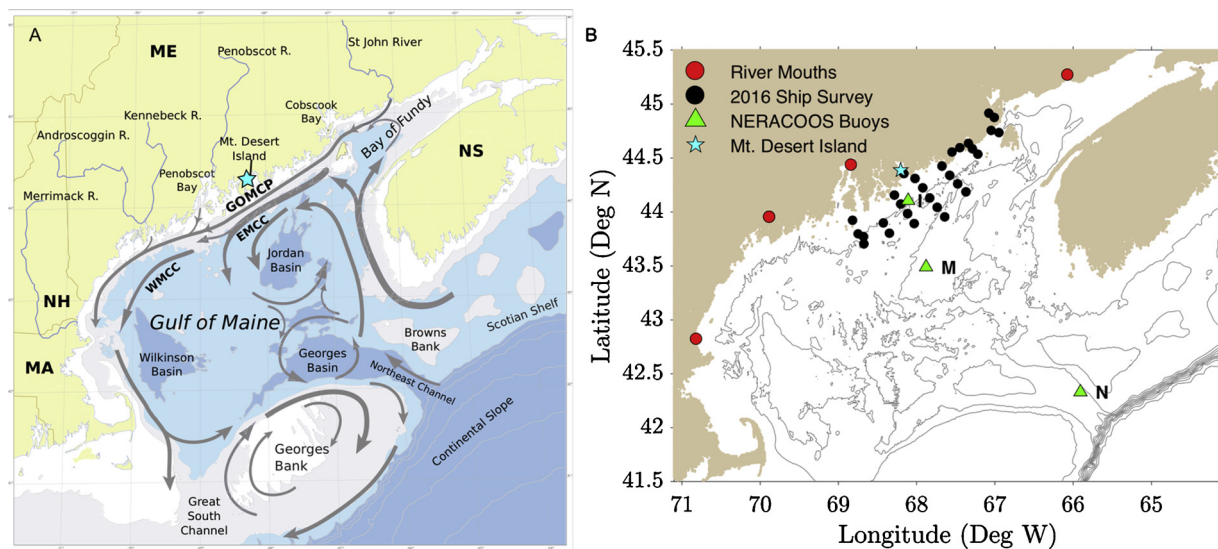
Fig. 1. (A) Climatological circulation of the GOM as described in Pettigrew et al. (2005) and adapted in Anderson et al. (2006) (Used with permission). GOMCP stands for Gulf of Maine Coastal Plume, WMCC stands for Western Maine Coastal Current, and EMCC stands for Eastern Maine Coastal Current. Two-letter abbreviations are for Massachusetts (MA), New Hampshire (NH), and Nova Scotia (NS). (B) Locations of hydrographic instruments and the 2016 *Pseudo-nitzschia* ship survey in the GOM. "Mt Desert Island" is shown, where both MDIBL and Bar Harbor are located.

2014 (Fernandes et al., 2014) and in 2016 an unprecedented bloom of *P. australis* led to the first regional observations of shellfish DA concentrations exceeding the regulatory limit of $20\,\mu g$ DA g^{-1} shellfish tissue (Bates et al., 2018). Beginning in mid-September, DA in shellfish tissue in the Bay of Fundy exceeded $18\,\mu g$ DA g^{-1} shellfish tissue and it remained elevated through the end of the month (Canadian Food Inspection Agency, 2016). Along the coast of Maine, clam and mussel harvesting was suspended sequentially from the northeast to the southwest, beginning with Cobscook Bay at the Canadian border on September 27, continuing to Mount Desert Island by September 30, and eventually growing to include Penobscot Bay by the first week of October (refer to Fig. 1 for location references) (Rappaport, 2016).

Threats to economic and human health, along with *Pseudo-nitzschia*'s apparent growing presence, have motivated studies about the factors – biogeochemical, ecological, and physical – controlling *Pseudo-nitzschia* blooms. Studies on *Pseudo-nitzschia* growth have argued that, because *Pseudo-nitzschia* are often lightly silicified relative to other diatoms, they are most competitive in waters with low silicate- (or silicic acid)-to-nitrate ratios (Marchetti et al., 2004; Parsons et al., 2002), in that they thrive when there is sufficient nitrogen to support protein synthesis, but too little silicic acid for other diatom species. Other studies have connected species-specific growth rates to specific temperatures (Santiago-Morales and García-Mendoza, 2011) or salinities (Doucette et al., 2008). *Pseudo-nitzschia* have been linked to hydrodynamic features, such as the Juan de Fuca Eddy, which acts as an incubation site for *Pseudo-nitzschia* blooms (Trainer et al., 2002). In the Santa Barbara Channel, convergent eddies were found to aggregate pre-existing, low density blooms until their densities increased from $5*10^5$ to more than $2*10^6$ cells L^{-1} (Anderson et al., 2006). Bloom development and transport has also been connected to wind direction and upwelling conditions in Washington (MacFadyen et al., 2005), California (Schnetzer et al., 2013), Portugal (Palma et al., 2010), and Ireland (Cusack et al., 2015).

Cell growth is not the only factor controlling DA concentrations in a *Pseudo-nitzschia* bloom: inter- and intraspecific variation in DA production depend on environmental conditions. DA production has been connected to iron limitation, low silicic acid concentrations, increased pH, increased salinity, the presence of predators, light availability, and sometimes even multiple, compounding factors (as reviewed in Bates et al., 2018; Trainer et al., 2012). In addition, laboratory studies do not always translate to the field, where multiple factors change

simultaneously and pathways towards DA production are complex. Several field studies have concluded that *Pseudo-nitzschia* DA production in the field cannot be attributed to one single environmental parameter (Smith et al., 2017; Trainer et al., 2009).

Pseudo-nitzschia in the GOM have not been extensively studied, but their growing presence and particularly the DA event in 2016 motivate the need to understand the dynamics of the genus in this region. DA poses a threat both to the economy and to human health. However, because of the disconnect between laboratory results and field observations, the varied theories about DA production, and the range of possible *Pseudo-nitzschia* growth conditions in the field, it is challenging to draw conclusions on *Pseudo-nitzschia* or DA dynamics based entirely on information from the literature.

This paper explores the biogeography of *Pseudo-nitzschia* species in the GOM from 2012–2016. Environmental factors controlling species composition and toxic *Pseudo-nitzschia* blooms are explored through descriptive and statistical analysis of genetic species, nutrient, and hydrodynamic data. The effects of environmental factors and species composition on DA are analyzed. Special attention is given to explaining the 2016 bloom and exploring factors that led to the highest pDA concentrations ever recorded in the GOM.

2. Methods

2.1. Study site

The GOM is a coastal sea on the North American East Coast that stretches from Cape Cod, Massachusetts at 42 °N to the Bay of Fundy at 44.5 °N (Fig. 1A). Mean sea surface temperature ranges from ~6 °C in February to ~22.5 °C in August, and salinity ranges from 29 to 33.5 (Li and He, 2014). The five largest rivers that feed into the GOM are, in order of decreasing volume flux, the St. John River, Penobscot River, Kennebec River, Androscoggin River, and Merrimack River (Li et al., 2014). Because of resonance of the M2 tide, the GOM is home to some of the largest tidal amplitudes in the world: tidal amplitudes at the northern end of the Bay of Fundy can reach 6 m (Lynch and Naimie, 1993). This tidal energy can fully mix the water column in the Northeastern Gulf, Bay of Fundy, Eastern Maine Coastal Current, and on the crest of Georges Bank, providing an important mechanism to transport nutrients to the surface (Townsend et al., 2014).

The GOM is comprised of three deep basins, Jordan Basin, Georges

Basin, and Wilkinson Basin, which are each deeper than 200 m. Exchange between the GOM and the Atlantic shelf sea is restricted by the shallow (< 100 m) Browns Bank and Georges Bank. Inflows occur via slope water from the North Atlantic entering through the Northeast Channel or Scotian Shelf Water flowing around the tip of Nova Scotia towards the Bay of Fundy, and outflows occur through both the South Channel and the Northeast Channel (Xue et al., 2000). The general circulation in the GOM is cyclonic, with anti-cyclonic flow around Georges Bank.

Alongshore transport in the GOM is driven by the coastal-trapped river plume and the Gulf of Maine Coastal Current (GMCC) (Bisagni et al., 1996; Pettigrew et al., 2005). The pressure-gradient-driven GMCC connects the eastern GOM to the western GOM, and has been shown to be important to *Alexandrium catenella* bloom dynamics (Keafer et al., 2005; Li et al., 2009), but the strength of the connection varies interannually (Pettigrew et al., 2005). As shown by McGillicuddy et al. (2011), several hydrodynamic processes, including upwelling winds, stratification, and alongshore transport, influence HAB dynamics in the GOM; anomalies in one process, in addition to biological factors, could create conditions for an extremely large bloom, or none at all.

2.2. Biological data – ship surveys

Shipboard surveys were conducted on the *R/V Tioga* on August 4th – 5th 2012, July 25th – 27th 2014, and August 2nd – 5th 2015, and on the *R/V Gulf Challenger* on October 5th – 7th 2016. Sample stations were arranged in offshore transects centered on Mount Desert Island, Maine, and extended up to 60 km offshore (Fig. 1B). The number and locations of sample stations varied depending on weather and in response to *Pseudo-nitzschia* bloom locations: 25 stations were sampled in 2012, 36 in 2014, 40 in 2015, and 21 in 2016. At each station, discrete water samples were collected with Niskin bottles at 1, 10, 20, 30, 40 and 50 + m (site depending). Casts with a CTD Sea-Bird 9 recorded temperature (ºC), salinity, conductivity (siemens m^{-1}), transmissivity ($1 m^{-1}$), turbidity (NTU), dissolved oxygen (ml L^{-1}), and pressure (dbar).

2.2.1. Pseudo-nitzschia data

Cell Counts. For cruise samples, 125 mL whole seawater samples from 1, 10, and 20 m were preserved with Lugol's fixative. A 3-mL aliquot was added to a 5-mL Nunc Lab-Tek 2-chamber counting chamber (ThermoFisher) and *Pseudo-nitzschia* cells were enumerated with a Zeiss Axiovert inverted light microscope at 200–400x magnification and categorized into two size categories, small (< 3 μm in width) and large (> 3 μm in width), and two orientations, chain or single-celled. In 2016, an intermediate size category (˜3 μm in width) was added. The limit of detection (LOD) for cell counts by light microscopy was 333 cells L^{-1}. Absolute cell abundance was recorded as the total of all sizes and cell orientations.

Relative Species Abundance. Water samples were also analyzed for species composition via Automated Ribosomal Intergenic Spacer Analysis (ARISA) (Hubbard et al., 2014). After filtration of 125 mL of seawater onto 0.45 μm pore size nitrocellulose filters (Millipore), filters were frozen shipboard with liquid nitrogen and stored at −80 °C until extraction. DNA was extracted with a DNeasy Plant Mini Kit (Qiagen Inc.), amplified via polymerase chain reaction (PCR) with the *Pseudo-nitzschia*-specific ITS1 primer set PnALL F/R, and purified using MultiScreen PCR 96 filter plates (Millipore) as described in Hubbard et al., 2014. For ARISA, PCR products were standardized and 1 ng DNA was analyzed on an ABI 3730 XL. Electropherograms were analyzed using DAx software (Van Mierlo Software Consultancy, Eindhoven, Netherlands) to characterize amplicon sizes (for species association) and relative peak heights (for quantitative assessments) according to Hubbard et al. (2014). Amplicon sizes characterized by ARISA were identified by comparing results with the GenBank nucleotide (nr/nt) database and regional studies (summarized in and including Fernandes et al. (2014)).

For the 2016 event, *P. australis* was identified using ITS1 sequencing (targeting the ARISA amplicon) of DNA from live chains (placed in 5 μL DNA-free water and subjected to three freeze-thaw cycles) and extracts used for ARISA (see Smith et al. (2017)). *P. australis* identification was confirmed with scanning electron microscopy conducted on Lugol's preserved material (Bates et al., 2018).

2.2.2. Particulate domoic acid

For pDA analysis, 125–250 mL of seawater were filtered through a 0.45 μm pore size nitrocellulose filter and frozen at -20 °C until analysis. Prior to analysis, extracts were filtered through 0.22 μm PVDF syringe filters. Extracts were analyzed using an Acquity UPLC system coupled to a Quattro Micro™ API triple quadrupole mass spectrometer operated in positive ionization mode (ESI +) according to a method adapted from Wang et al. (2007). Separations were performed on an Acquity UPLC BEH C18 1.7 μm column (2.1 x 50 mm). Mobile phase consisted of Nanopure water (A) and acetonitrile (B) in a binary system with 0.1% formic acid as an additive. The detection of domoic acid was achieved by multiple reaction monitoring (MRM) using optimized instrument parameters. MRM transitions from the protonated DA ion were monitored for the following transitions: m/z 312 > 248, and m/z 312 > 266 and m/z 312 > 193. The transition m/z 312 > 266 was used for quantitation. A certified reference solution of domoic acid purchased from the National Research Council, Halifax, Canada was used to generate a 9-point standard curve from 0.78 to 200 ng DA mL^{-1}. The limit of detection was defined as the level yielding a signal to noise ratio of 3. The limit of quantitation was defined as the lowest concentration on the standard curve (0.78 ng DA mL^{-1}) or the concentration that yielded a signal to noise ratio of 10 if that was greater than 0.78 ng DA mL^{-1}.

2.3. Biological data – Mt. Desert Island time series

From 2013 to 2016, weekly water samples were collected from Mt. Desert Island Biological Laboratory (MDIBL) and Bar Harbor on Mt. Desert Island, Maine as part of the Maine Department of Marine Resources' volunteer phytoplankton monitoring program. Ten-liter water samples were concentrated to 15 mL using a 15 μm sieve, which may not have captured all (especially smaller) *Pseudo-nitzschia* cells. For cell counts via light microscopy, a 1 mL sample was added to a gridded Sedgewick Rafter slide, and cells L^{-1} were enumerated either by counting all cells or by estimating based on the grid number at which 500 cells were enumerated; cells were categorized as either "large" (> 3 μm in width) or "small" (< 3 μm in width). Species composition at Bar Harbor in 2013 was evaluated by ARISA (Section 2.2.1) and pDA was measured from whole seawater by LC–MS/MS (Section 2.2.2). Water temperature, salinity, and dissolved oxygen were measured with a handheld YSI (YSI Instruments, Yellow Springs, OH), and dissolved nutrient concentrations were measured from whole seawater samples according to the methods in Section 2.4.

2.4. Physicochemical data

Nutrients. Ship survey water samples from 1, 10, and 20 m and Mt. Desert Island surface samples were analyzed for nitrate + nitrite (NO_x^-), ammonium (NH_4^+) silicic acid ($Si(OH)_4$), and phosphate (PO_4^{3-}). Samples were filtered through a 0.22 μm acetate luer-lock syringe filter and frozen at -20 °C until analysis. Dissolved NO_x^-, phosphate, and silicic acid concentrations were measured with a QuickChem 8500 Flow Injection Analysis system, and dissolved ammonium concentrations were measured on a TD-700 fluorometer.

Oceanographic, Atmospheric, and Riverine Measurements. Buoys from the Northeastern Regional Association of Coastal Ocean Observing Systems (NERACOOS) have recorded temperature, salinity, conductivity, potential temperature, air temperature, air pressure, and wind speed at hourly intervals since 2001 (Morrison, 2019) (Fig. 1B).

Instruments were positioned at 1, 20, and 50+ m below the surface (site-depending), allowing for characterization of the vertical structure of the water column at high temporal resolution. Salinity and temperature data from buoys N, M, and I from 2001–2016 were used to characterize water mass characteristics and climatology. Wind speed and direction from station I were used to calculate the upwelling index from 2001 to 2016.

An upwelling index (UI) was calculated according to Schwing et al. (1996): $UI = \frac{\tau_x}{\rho f}$, where τ_x is the alongshore component of the wind stress as defined by Large and Pond (1981), ρ is the surface water density in kg m^{-3}, and f is the Coriolis parameter. According to this convention, a positive UI indicates upwelling, while a negative UI indicates downwelling. Cumulative UI (CUI) was calculated by integrating UI over time from April through December in each year from 2001 to 2016.

The U.S. Geological Survey (USGS, 2013) and Canadian Water Office (Canada, 2018) report daily mean river discharge (m^3 s^{-1}) for the St. John, Penobscot, Kennebec, Androscoggin, and Merrimack rivers. Cumulative river discharge was calculated in 2012–2016 by integrating daily discharge in m^3 s^{-1} over time to calculate m^3.

Data used for this study are summarized in Table 1.

2.5. Descriptive and statistical analyses

Cell concentrations and species relative abundance were plotted at their sample locations to explore spatial variability. Each analysis described below was conducted on absolute cell abundance (cells L^{-1}), relative species abundance, chlorophyll, pDA, temperature, salinity, and dissolved nutrient concentrations. Relative nutrient concentrations were also analyzed including the silicic acid-to-total nitrogen ratio (Si(OH)$_4$:(NO$_x^-$ + NH$_4^+$) or simply Si:N), silicic acid-to-phosphorous ratio (Si(OH)$_4$:PO$_4^{3-}$ or Si:P), total nitrogen-to-phosphorous ratio ((NO$_x^-$ + NH$_4^+$):PO$_4^{3-}$ or simply N:P), and residual silicic acid ($Si^* = [Si(OH)_4] - [NO_x^-]$). Each year was analyzed individually, with all depths combined, except where indicated otherwise. For all statistical tests, correlations with a p-value < 0.05 were considered significant.

ARISA data were used in conjunction with pDA concentrations to estimate cellular DA (DA cell^{-1} or cDA), which varies widely among *Pseudo-nitzschia* species and is thus challenging to estimate from field data. Therefore, samples dominated by one species (relative abundance > 85%) were selected, with exceptions made for samples as low as 70% relative abundance of the dominant species, as long as the other species were not associated with pDA in the dataset. Such allowances increased the number of samples to improve statistical robustness. If a sample had > 85% relative abundance from the dominant species, but *P. australis* was also detected by ARISA, then that sample was discarded because *P. australis* is known to produce pDA. PDA (g L^{-1}) was divided by the total cell concentration (cells L^{-1}) to find an estimate of cDA (pg cell^{-1}). The cDA calculation accounted for the relative abundance of the dominant species by dividing by its fraction of the sample:

$$\frac{DA}{cell} = \frac{pDA \ (Water \ Volume)^{-1}}{(relative \ abundance) * (cells \ (Water \ Volume)^{-1})}$$

Correcting by the relative abundance makes the assumption that DNA

prevalence is proportional to cell counts, which is not necessarily correct. However, the calculation was also performed without adjusting for relative abundance, and the results varied little. The calculation was also performed with a lower minimum cutoff for relative abundance of the dominant species of 60%, and the main results did not change (refer to supplementary material).

Several statistical analyses were employed to quantify the relationships observed in the descriptive analysis. Linear least squares regression was used to explore correlations between species relative abundance, cell abundance, pDA and environmental parameters. Each species was tested against the environmental factors listed at the beginning of this section. Regression analysis was run for the cruise data and time series data, with each year individually, with all years combined, with all samples, and with only samples where pDA > LOQ.

Principal Component Analysis (PCA) was used to quantify variability in environmental factors and species relative abundance in the cruise data. Canonical Correspondence Analysis (CCA) was used to quantify correlations between environmental factors and community species composition in the cruise data. PCA and CCA were performed both on each year individually and on all years combined.

Lastly, the Wilcoxon signed rank test was used to test whether the measured environmental factors were statistically significantly different between years. This test was chosen because it does not assume normal sample distribution. Cruise data from 2016 were compared with other cruise data (2012, 2014, and 2015). Samples with pDA > LOQ were used, as the goal was to determine the effect of different environmental factors on DA concentrations when toxic species were already present.

3. Results

3.1. Biogeography prior to 2016

3.1.1. Temporal variability

Pseudo-nitzschia dynamics in the GOM exhibited interannual and seasonal variability in bloom timing, cell abundance, and relative species abundance (Figs. 2 and 3). Notable patterns are summarized below.

Interannual Variability. Maximum cell abundance was 75,000 cells L^{-1} in 2012, 190,000 cells L^{-1} in 2013, 65,000 cells L^{-1} in 2014, and 180,000 cells L^{-1} in 2015. Ten *Pseudo-nitzschia* species were present in the GOM from 2012 to 2015, based on ARISA and sequencing data: *P. pungens*, *P. plurisecta*, *P. seriata*, and *P. delicatissima* were consistent members of the community, with varying degrees of relative abundance, while *P. multiseries*, *P. heimii/americana*, *P. fraudulenta*, *P. cuspidata*, *P. caciantha*, and *P. obtusa* were detected only in some years (Table 2). Before 2016, GOM interannual variability was characterized by shifts in dominance between four species, but not complete shifts in species assemblage. In addition, while some samples were dominated by one species, in none of the years prior to 2016 was a single species dominant in all samples for that year.

Seasonal Progression. Temporal variability also existed in the form of seasonal progression. Based on the monitoring time series from MDIBL, there were two *Pseudo-nitzschia* cell concentration peaks in 2013 with varying species composition. The first peak of 150,000 cells L^{-1} occurred in late-July/early-August and was comprised largely of *P.*

Table 1

Summary of physical and biological time series and survey data. MDIBL = Mt. Desert Island Biological Laboratory; NO$_x^-$ = nitrate + nitrite; NH$_4^+$ = ammonium; Si(OH)$_4$ = silicic acid; PO$_4^{3-}$ = phosphate.

| Data Description	Sample Dates	Parameters
Survey Cruises	Aug 2012, Jul 2014, Aug 2015, Oct 2016	Temperature, Salinity, NO$_x^-$, NH$_4^+$, Si(OH)$_4$, PO$_4^{3-}$, *Pseudo-nitzschia* cell counts, Species Relative Abundance
MDIBL time series	Jul-Nov 2013, Jun-Oct 2014, Feb-Sep 2015, Jun-Oct 2016	All years: *Pseudo-nitzschia* cell counts 2013 only: Temperature, Salinity, NO$_x^-$, NH$_4^+$, Si(OH)$_4$, PO$_4^{3-}$, Species Relative Abundance
NERAOCOS moorings	Continuous 2002-2017	Temperature, Salinity, Air temperature, Air Pressure, Wind Speed
River Gauges	Varied	Daily discharge
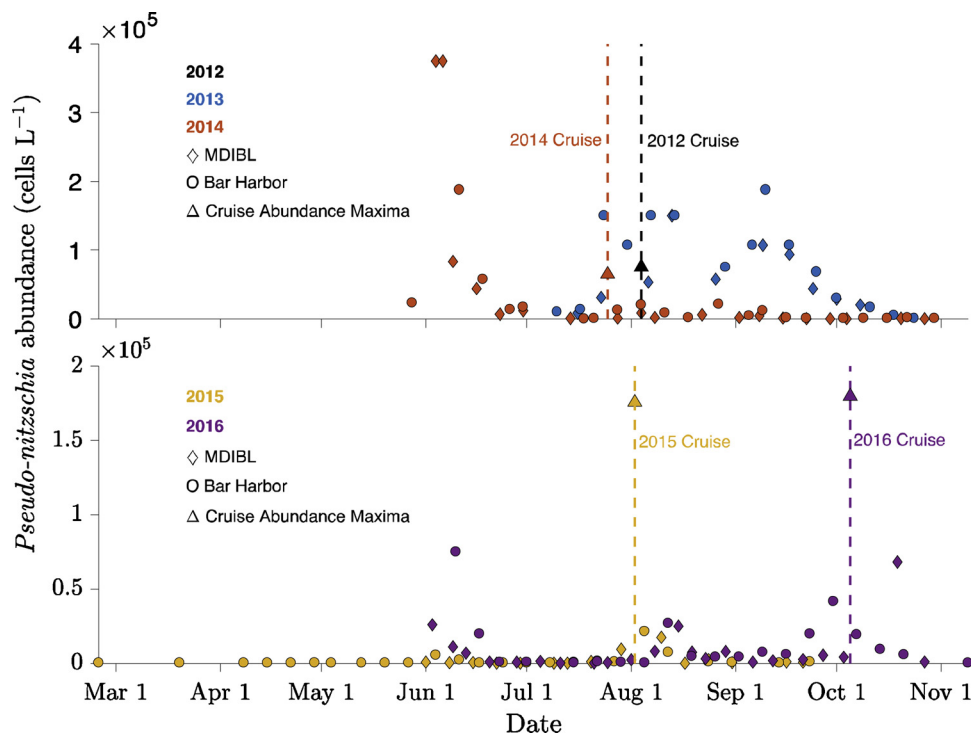
Fig. 2. From the MDIBL and Bar Harbor time series data, *Pseudo-nitzschia* spp. cell concentration versus time in 2013, 2014, 2015, and 2016. Timing of the 2014, 2015, and 2016 cruises are indicated with vertical lines. Maximum total cell abundance from each cruise is plotted as a single point. Note that the y axis scales are different.

plurisecta (Fig. 3). The second peak of 190,000 cells L^{-1} occurred in mid-September and included mostly *P. pungens*.

3.1.2. Spatial variability

In addition to temporal variability, spatial variability was observed in the cruise data (Figs. 4–7). Prior to 2016, the greatest cell concentrations were consistently inshore and at the surface. Because the inshore waters also had lower salinity, the samples in 2012 and 2015

could be categorized into two groups: one group at higher salinity and lower cell counts (offshore), and the second group at lower salinities and higher cell counts (inshore).

In 2012, inshore salinity ranged from 31.5 to 32.5 while offshore salinity ranged from 32.5 to 33.5 (Fig. 4). In 2015, inshore salinity ranged from 29 to 32.5, while offshore salinity ranged from 32 to 33 (Fig. 6). *P. plurisecta* was consistently found at greater relative abundance in inshore samples, while *P. seriata* and *P. delicatissima* were
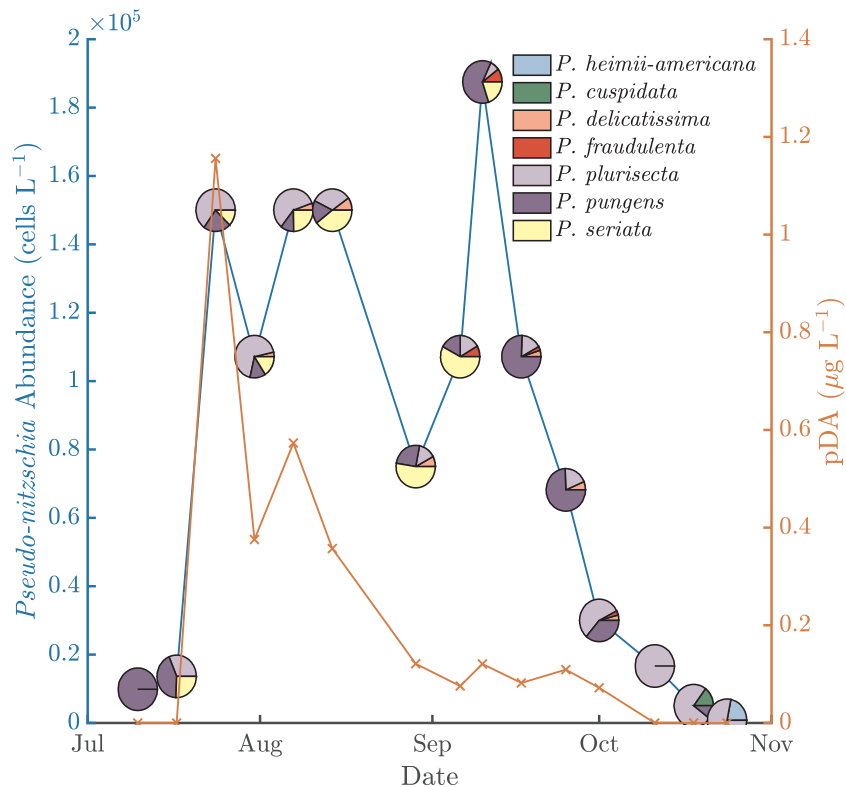

Fig. 3. From the Bar Harbor time series, *Pseudo-nitzschia* cell concentration (left axis; blue line) and pDA (right axis; red Xs) versus time in 2013. Relative species abundance for each sample is indicated with pie charts (For interpretation of the references to colour in this figure legend, the reader is referred to the web version of this article).

Table 2
Presence/Absence of Pseudo-nitzschia species 2012-2016. An 'X' indicates that in at least one sample the ARISA measured > 0 relative abundance for that species in that year.

	P. delicatissima	P. plurisecta	P. pungens	P. seriata	P. australis	P. caciantha	P. cuspidata	P. fraudulenta	P. heimii/americana	P. obtusa
2012	X	X	X	X			X		X	X
2013	X	X	X	X			X	X	X	X
2014	X	X	X	X		X	X			
2015	X	X	X	X		X	X	X	X	
2016	X	X	X	X	X			X	X	

consistently found in offshore samples (Figs. 4 and 6). *P. pungens* was found both inshore and offshore.

3.2. 2016 event

In 2016 shellfisheries were closed because shellfish DA concentrations exceeded the regulatory limit for the first time in the GOM (Bates et al., 2018). Particulate DA concentrations reached a maximum of 37.5 μg L^{-1} at one site and were on average an order of magnitude larger than pDA measured in previous years (Fig. 8). Shellfishery closures in the GOM were preceded by shellfishery closures in the Bay of Fundy, where shellfish DA concentrations exceeded 20 μg of DA g^{-1} shellfish tissue at various locations from September 16 to 30 (Canadian Food Inspection Agency, 2016).

The 2016 bloom likely began in September in the Bay of Fundy, and samples containing up to 180,000 *Pseudo-nitzschia* cells L^{-1} were collected along the Eastern Maine coast during the 2016 cruise from October 5 to October 7. The bloom was accompanied by greater salinity, greater ammonium, and lower Si*, all of which were significantly different from measurements in at least one previous year (Section 3.4).

During the 2016 bloom, *P. australis* was observed at all sample sites and depths (Fig. 7), and therefore at varying nutrient ratios and the full range of temperatures (12.23–14.20 °C) and salinities (32.77–33.61) recorded that year. The inshore-offshore biogeographic patterns in cell abundance and species composition that were observed in summer 2012 and 2015 (Section 3.1) were not present in fall 2016. Cell abundances and *P. australis* relative abundance were relatively uniform across the sample area from inshore to offshore.

3.3. Domoic acid

DA concentrations varied spatially, seasonally, and interannually, in correlation with cell concentrations and with the relative abundance of known toxic species (Fig. 9). In 2012, the highest pDA (0.06 μg L^{-1}) was observed in samples with at least 10^4 cells L^{-1} and > 50% *P. plurisecta* relative abundance. At Mt. Desert Island in 2013, the first peak in cell abundance, which was dominated by *P. plurisecta*, a known toxic species, coincided with a peak in pDA (Fig. 3). The second peak, however, which was dominated by *P. pungens*, did not result in elevated DA concentrations. In 2014, relative species proportions were constant, but pDA concentrations increased as absolute cell concentrations increased: the maximum pDA (0.23 μg L^{-1}) co-occurred with a cell concentration of 15,000 cells L^{-1}, and most pDA concentrations over 0.1 μg L^{-1} co-occurred with cell concentrations greater than 10^4 cells L^{-1}. In 2015, samples with *P. plurisecta* had higher pDA than those with *P. delicatissima* and *P. seriata*, and the greatest pDA concentration was 0.31 μg L^{-1}. In 2016 the greatest pDA concentration was 37.5 μg L^{-1}, and samples that were nearly completely dominated by *P. australis* had the greatest pDA.

Estimated cDA varied widely in the survey and time series data. From samples dominated by one species, cDA estimates were possible for *P. australis*, *P. pungens*, *P. seriata*, *P. delicatissima*, and *P. plurisecta*. PDA was < LOQ in all samples dominated by *P. delicatissima*. Cellular DA estimates were < LOQ–11.1 pg cell^{-1} for *P. seriata*, 0.6–26.7 pg cell^{-1} for *P. plurisecta*, and 10.2–42.6 pg cell^{-1} for *P. australis* (more information can be found in the supplementary material). *P. pungens* cDA estimates were only greater than zero when the analysis was run including samples with relative abundance as low as 60%, and ranged from < LOQ–0.75 pg cell^{-1}. This approach was validated by
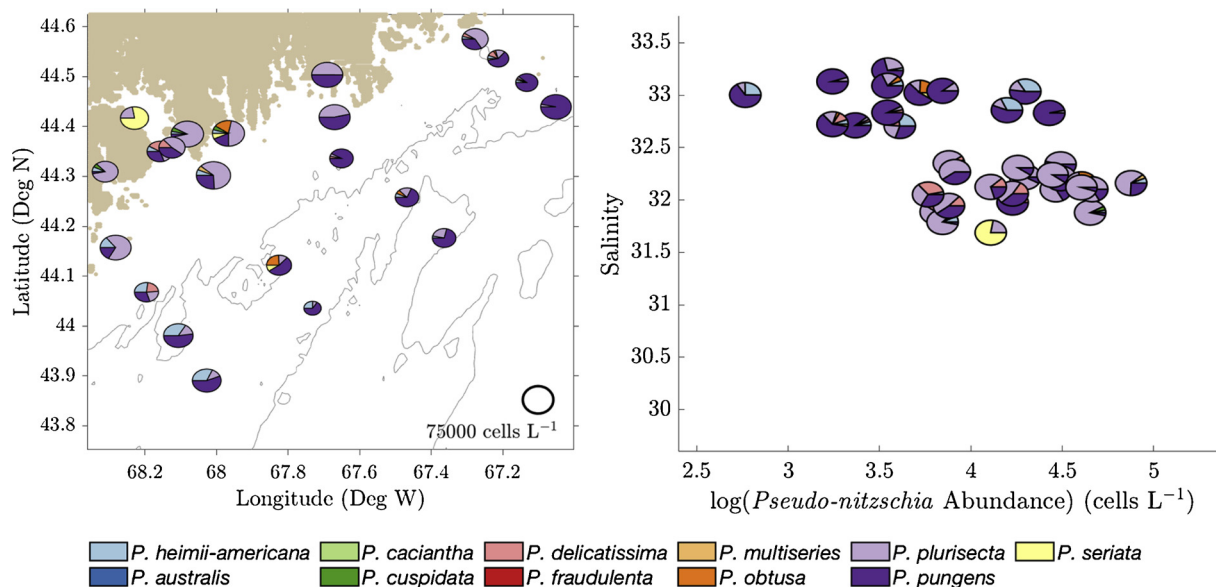

Fig. 4. (Left) August 2012 species relative abundance of surface samples plotted on the sampling locations in the GOM. Pie chart size was determined by log(cell count) (scale shown at lower right). (Right) 2012 relative species abundance on a salinity vs. cell count diagram, with axes scaled to match Figs. 5–7.
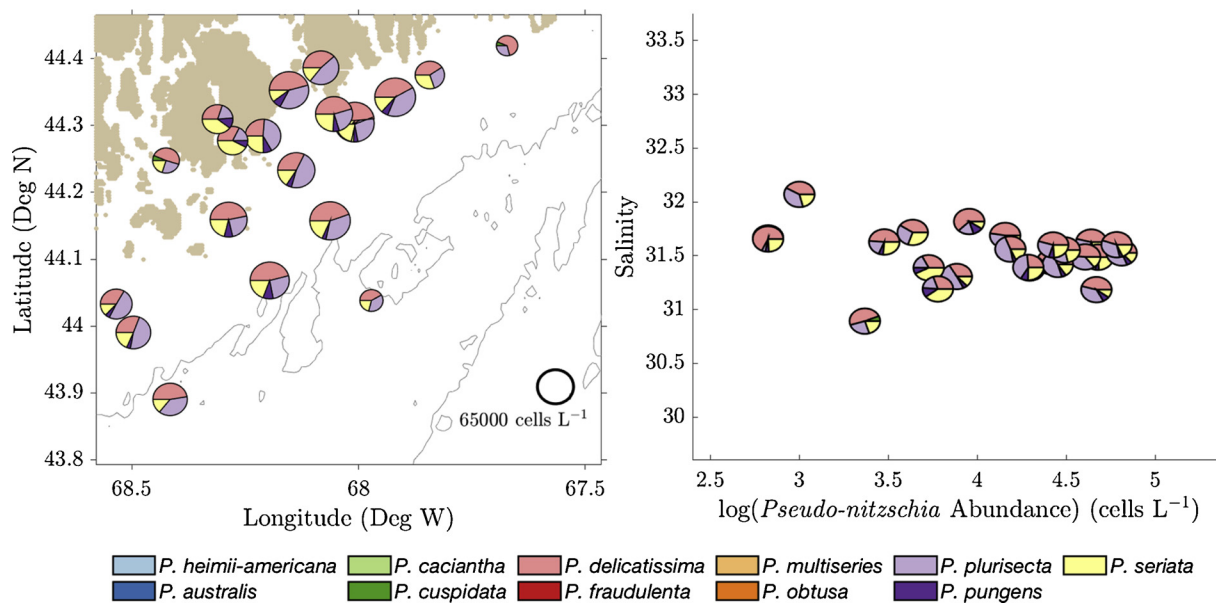
Fig. 5. (Left) July 2014 species relative abundance of surface samples plotted on the sampling locations in the GOM. Pie chart size was determined by log(cell count) (scale shown at lower right). (Right) 2014 relative species abundance on a salinity vs. cell count diagram, with axes scaled to match Figs. 4–7.

previously published estimates for the observed species: cDA estimates for *P. pungens* and *P. delicatissima* are less than 1 pg cell^{-1}, while cDA estimates for *P. seriata* range from 0.8 to 33.6 pg cell^{-1} (Trainer et al., 2012). *P. plurisecta* was previously identified and confirmed to produce DA in the GOM (Fernandes et al., 2014), and *P. australis* cDA has been shown to reach > 90 pg cell^{-1} (Ryan et al., 2017).

3.4. Statistical analysis

Statistics were used to quantify correlations from the descriptive analysis, beginning with correlations with environmental parameters. Linear regressions between pDA concentrations or relative species abundance and environmental parameters yielded statistically significant results (p-value < 0.05), however the correlations were low (R^2 < 0.1). The exception is in linear regressions from 2013: *P. pungens* was negatively correlated with temperature (R^2 = 0.85), *P. seriata* was negatively correlated with salinity (R^2 = 0.53), and pDA was negatively correlated with phosphate (R^2 = 0.57). Some correlations existed between relative species abundance and salinity, which are discussed in

Section 3.1.2. When the analysis included only samples with pDA > LOQ (130 out of 372 total samples), pDA and species abundance were not consistently correlated with one environmental parameter across the years. Thus, variabilities in species composition and pDA concentrations were not functions of any one environmental parameter. (Refer to supplementary material for full table of p-values and R^2 values from regression analysis.)

Linear regressions between relative species abundance and pDA were similarly inconclusive: R^2 values were less than 0.2. Therefore one species was not the sole producer of pDA across all years of the study. However, when the analysis included only samples with pDA > LOQ, there were consistent correlations between pDA and the relative abundance of *P. plurisecta*, *P. pungens*, *P. australis*, and total cell counts (Table 3).

CCA and PCA analyses were inconclusive: in neither of the analyses, whether each cruise individually or all cruises combined, were species clearly and consistently correlated with an environmental factor. From the analysis, nutrient and temperature variability dominated the system, but did not correlate with species variability. Despite a lack of
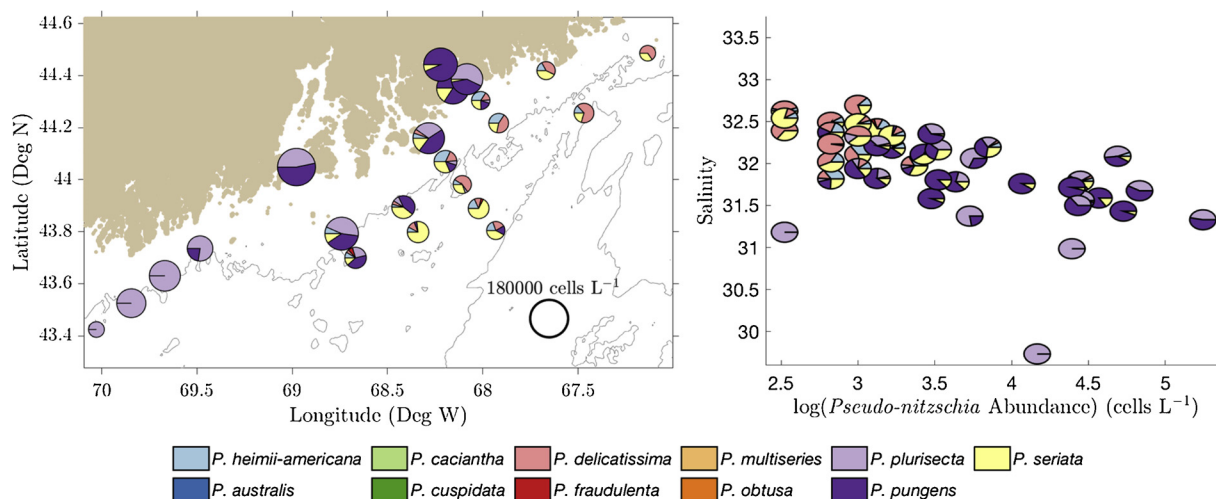

Fig. 6. (Left) August 2015 species relative abundance of surface samples plotted on the sampling locations in the GOM. Pie chart size was determined by log(cell count) (scale shown at lower right). (Right) 2015 relative species abundance on a salinity vs. cell count diagram, with axes scaled to match Figs. 4–7.
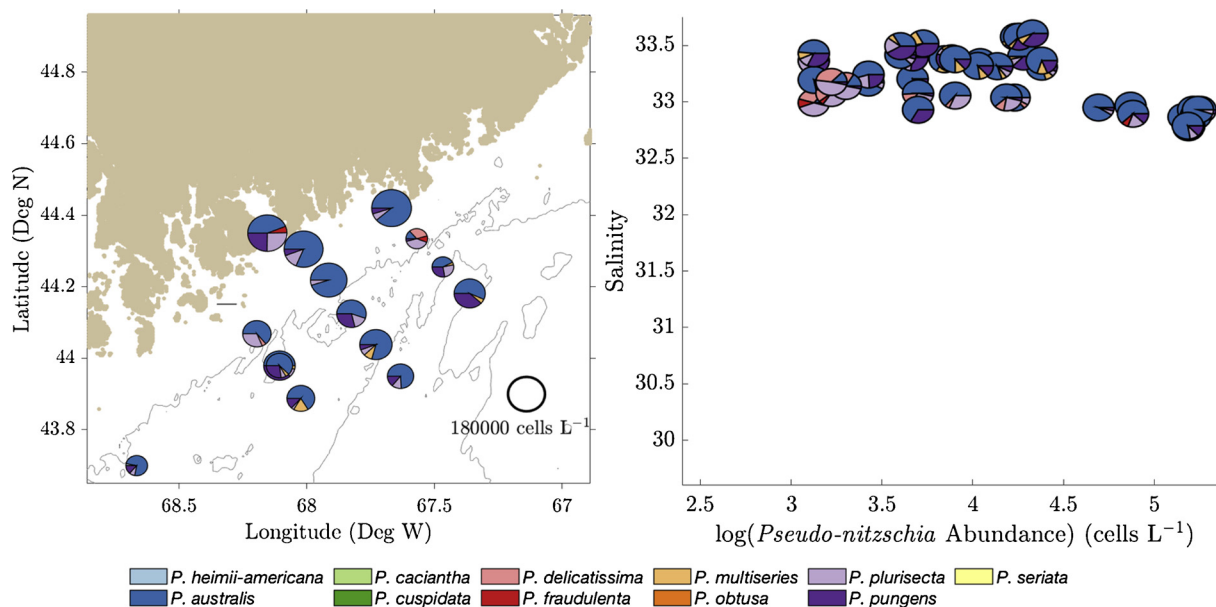
Fig. 7. (Left) October 2016 species relative abundance of surface samples plotted on the sampling locations in the GOM. Pie chart size was determined by log(cell count) (scale shown at lower right). (Right) 2016 relative species abundance on a salinity vs. cell count diagram, with axes scaled to match Figs. 4–6.
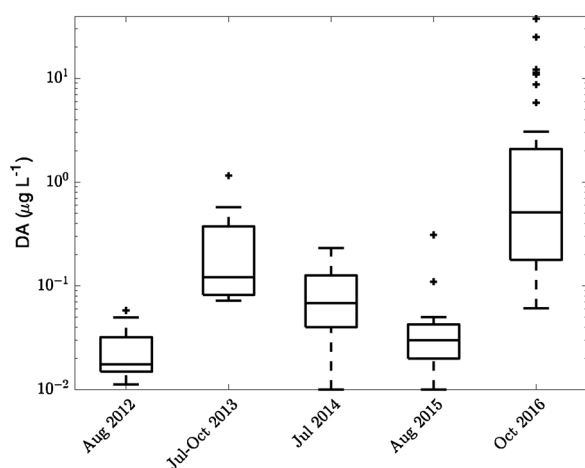

Fig. 8. Box-and-Whisker plots of particulate DA measured during August 2012, June-October 2013, July 2014, August 2015, and October 2016. Note that the y axis is a log scale. The crosses are outliers, defined as points greater than (less than) Q3(Q1) +(-) 1.5*(Q3-Q1), where Q1 is the first quartile and Q3 is the third quartile.

direct correlations between environmental factors and species or pDA, interannual differences were observed. According to the Wilcoxon signed rank test, ammonium, N:P, and salinity were significantly higher in 2016 than in 2012 and 2015, while Si* and Si:N were significantly lower in 2016 compared to 2012 and 2015. 2016 was not significantly different from 2014 in any category except cDA.

3.5. Physical forcing and hydrodynamics

The CUI in 2016 was at a minimum in May and increased faster in summer 2016 than in summer 2012, 2013, 2014, or 2015 (Fig. 10). By late September 2016, the CUI was larger than in all previous years except 2013, and an abrupt shift to downwelling-favorable winds occurred from the 23rd to the 27th of September. Cumulative river discharge was lower than the average from the 2001–2015 climatology (supplementary materials), and salinities during the 2016 cruise were higher and had a narrower range than in previous cruises (Fig. 10). North Atlantic inflows in 2016 were also noteworthy: at NERACOOS

Station M in 2016 there was a warm and salty anomaly at 250 m that caused salinity to increase from 34.25 to 34.8 and temperature to increase from 8.71 to 10.35 °C in 6 days (Fig. 11).

4. Discussion

### 4.1. Pseudo-nitzschia biogeography

Although inshore-offshore *Pseudo-nitzschia* biogeography correlated with salinity, it may not be due to differences in species' salinity preferences. In fact, the literature is inconsistent on salinity preferences for species in the dataset. For example, *P. delicatissima* and *P. pungens* were observed in salinities ranging from 20.8 to 38 in the western Mediterranean (Quijano-Scheggia et al., 2008), while a survey of the Bay of Seine (Thorel et al., 2017) found a trend that was the opposite: *P. pungens* was found in 32–33.5 salinity waters, while *P. delicatissima* was found in 31.6–32.8 salinity waters.

Cross-shore patterns could also be indicative of underlying water mass changes. For example, inshore-offshore patterns in species composition have been observed in Monterey Bay, where an upwelled cold tongue divided non-toxic inshore populations of *P. fraudulenta* from toxic offshore populations of *P. australis* (Bowers et al., 2018). In the GOM dataset, cross-shore patterns in species composition and salinity may reflect the coastal river plume decreasing salinity in the nearshore, which was apparent in 2012 (Fig. 4) and in 2015 (Fig. 6). If variations in salinity are associated with different water masses, other factors likely varied simultaneously. Species' niche in salinity space was inconsistent from year to year in the GOM dataset, there are not currently enough data to tease apart the effects of only salinity from other factors, and seemingly contradictory findings in the literature may indicate intraspecific diversity. It is therefore not possible to define salinity niches in the GOM dataset.

4.2. Cruise results in the context of temporal variability

It may be tempting to draw conclusions about species' environmental preferences by comparing cruise data, but in each year the cruise data captured only a snapshot of a spatially and temporally variable process. It is therefore difficult to say what conditions preceded a bloom and how the bloom itself may have altered its environment. In
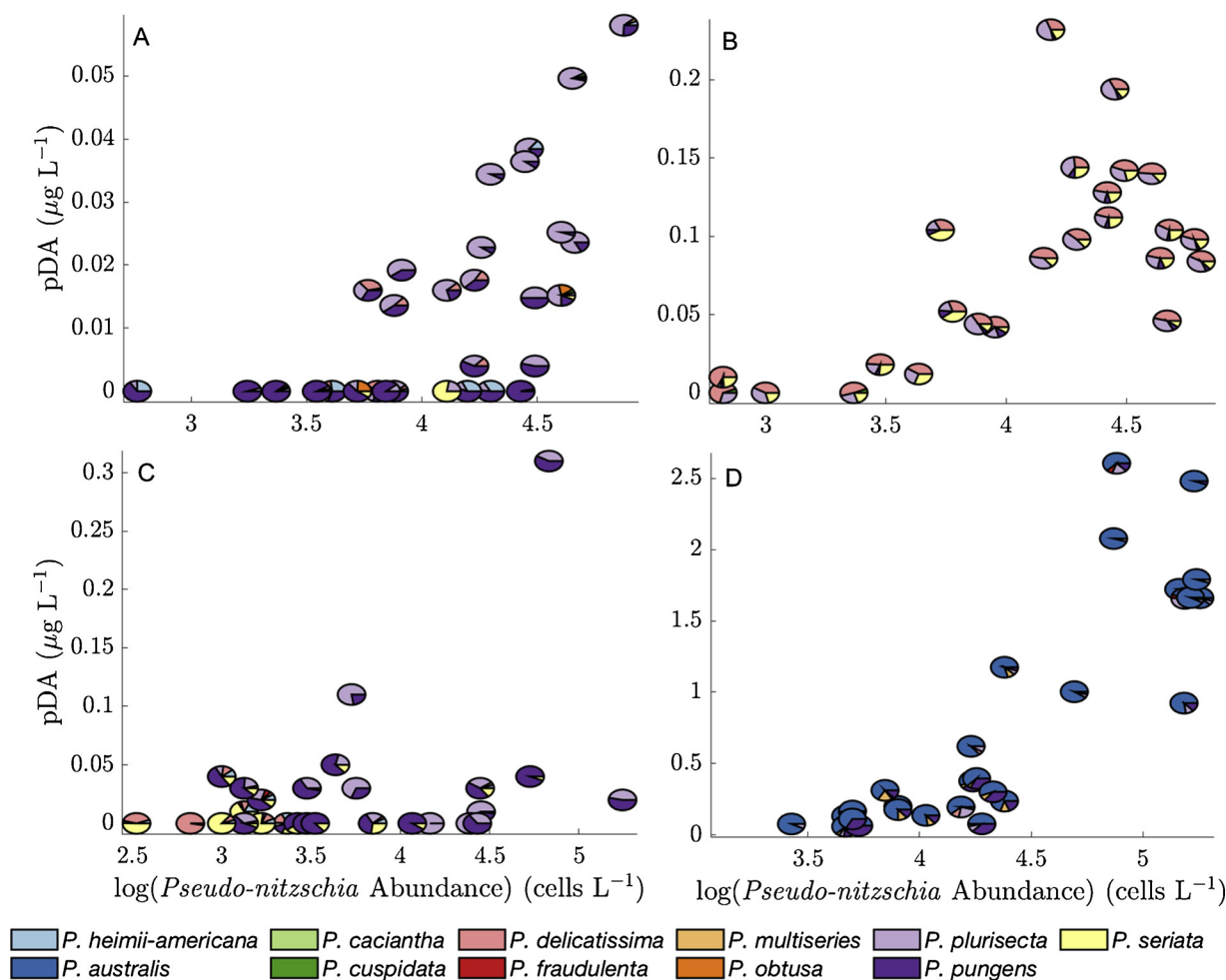
Fig. 9. Relative species abundance for each survey cruise on a particulate DA vs log(cell count) diagram: (A) 2012, (B) 2014, (C) 2015, (D) 2016. Note that the axes scales are not constant.

Table 3
Results of linear regressions between species abundance and pDA concentrations of only samples where pDA > LOQ`. Only statistically significant correlations of species with DA cell^{-1} > 0 are shown.

Year(s)	Species	R^2
2012	*P. plurisecta*	0.33
2012	Total cell count	0.47
2013	*P. plurisecta*	0.53
2014	*P. plurisecta*	0.29
2014	Total cell count	0.17
2016	*P. australis*	0.22
2016	Total cell count	0.66
2012-2016	*P. australis*	0.19
2012-2016	Total cell count	0.53

addition, seasonal progression in species relative abundance (e.g. 2013, Fig. 3) combined with interannual variability in the timing of peak cell abundance (Fig. 2), make it unlikely that four different cruises conducted at different times captured the same point in the blooms' progression. Variations among years therefore cannot be used to draw conclusions about factors regulating species distribution.

In 2014, inshore-offshore patterns were less pronounced than in 2012 and 2015. One explanation for this is interannual variability in species dominance, which has also been observed in the Bay of Seine: a 2012 bloom was a composite of *P. australis*, *P. pungens*, and *P. fraudulenta*, but a 2013 bloom was dominated by *P. delicatissima* (Thorel et al., 2017). However, because the same species were present in the GOM in

2012, 2014, and 2015, but at varying relative abundances, it is more likely that the difference in biogeography is due to differences in cruise timing relative to bloom timing and seasonal cycles in environmental conditions. The 2014 survey occurred when Bar Harbor and MDIBL cell concentrations were low, and *P. plurisecta* was observed in similar proportions across most sample sites. The 2012 and 2015 cruises, meanwhile, occurred when cell concentrations were at a maximum, and *P. plurisecta* dominated inshore (Fig. 2). In 2013, species assemblage shifted from a more even distribution early in the season to dominance by *P. plurisecta* later in the season (Fig. 3). Similar seasonal transitions have been observed in the English Channel (Downes-Tettmar et al., 2013) and western Scottish waters (Fehling et al., 2006): multiple species existed at one location, but they bloomed at different times of the year. Assuming the temporal pattern observed in the 2013 time series was consistent for the years preceding 2016, the cruises likely captured inshore summertime *P. plurisecta* dominance in 2012 and 2015 but not in 2014.

4.3. Domoic acid

The production of DA in the ocean depends both on the presence/abundance of a toxic species and on conditions that lead to DA synthesis. Genetic analysis confirmed the presence of certain species and pDA in each of the sampling years: *P. plurisecta* and *P. seriata* from 2012 to 2015, and *P. plurisecta*, *P. seriata*, and *P. australis* in 2016. In the cruise samples and MDIBL time series pDA typically increased with increasing relative abundance of *P. plurisecta* and *P. australis*, known DA-producers
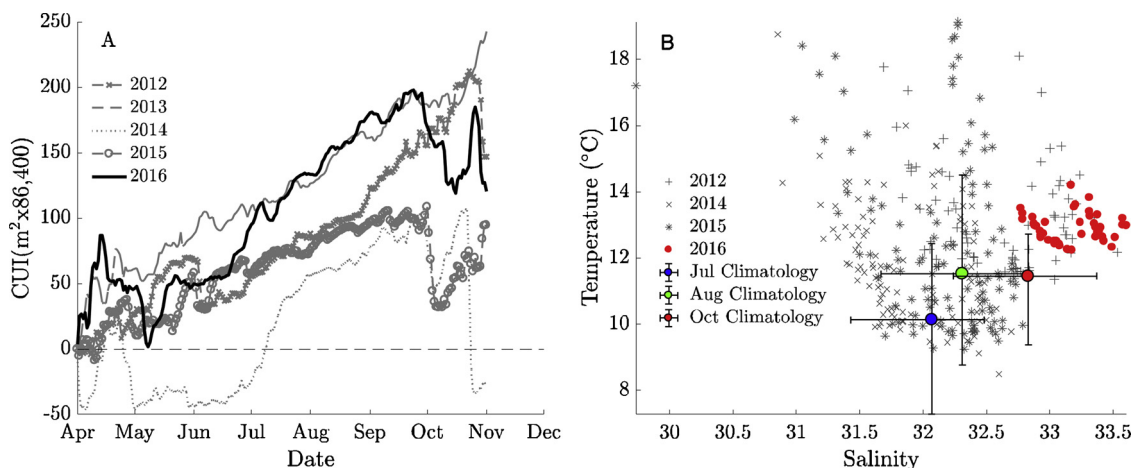
Fig. 10. (A) Cumulative Upwelling Index vs time in 2012–2016, calculated with atmospheric data from NERACOOS Station I. (B) Temperature and salinity measurements from all ship surveys plotted on one temperature-salinity diagram. Climatological means (circles) and minima/maxima (error bars) of temperature and salinity for the months July, August, and October (the same months as the cruise surveys) are also shown from NERACOOS station I.
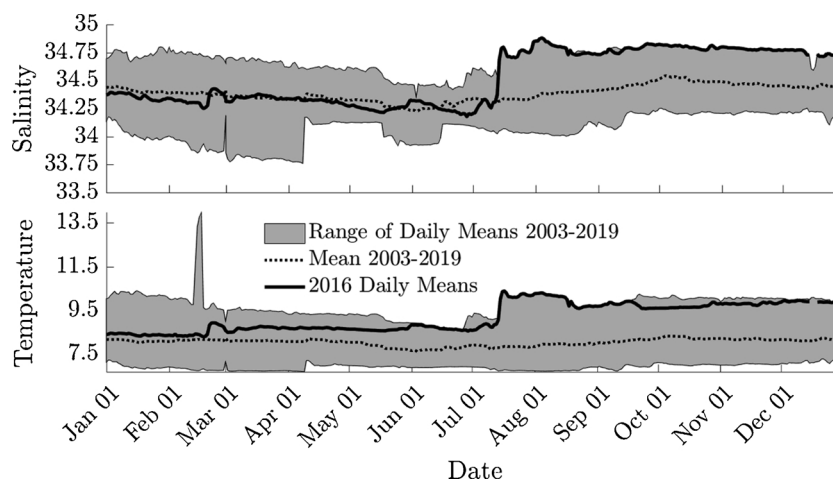

Fig. 11. Salinity (top) and temperature (bottom) climatology as measured by NERACOOS buoy station M (Jordan Basin) at 250 m. Climatology was calculated from data measured in 2003–2019, and 2016 daily means are overlain.

(Figs. 3 and 9). In 2016, when the species assemblage was dominated by the putatively toxic *P. australis*, pDA levels were an order of magnitude higher than previous years. In samples where pDA > LOQ, pDA was correlated with *P. pungens, P. plurisecta, P. australis* and total cell counts. Cellular DA calculations varied between species (Section 3.3), with highest cDA estimates for *P. australis* cells, followed by *P. plurisecta*, and finally *P. seriata* and *P. pungens*. Particulate DA concentrations were correspondingly highest in *P. australis*-dominated samples, followed by *P. plurisecta* samples, and *P. seriata* samples.

The effect of species composition on DA concentrations is supported by studies in both the field and the lab. In the Bay of Seine, Thorel et al. (2017) observed that blooms dominated by *P. delicatissima* were nontoxic, while blooms dominated by *P. australis* were toxic. That study reported variability in species composition, nutrient concentrations, nutrient ratios, salinity, temperature, and irradiance, but concluded that, of all these, species composition had the largest effect on DA. Similarly, Downes-Tettmar et al. (2013) observed seasonal variations in DA and species composition in the Western English Channel and concluded that DA concentrations correlated with cells from the *P. seriata* group (of which *P. australis* is part) and *P. pungens/multiseries* group. Lab studies have led to similar conclusions. Lema et al. (2017) measured the effects of varying phosphorus concentrations and changing species composition on DA production and concluded that species was the leading order factor to DA production. Based on cDA analysis, linear

regressions, and evidence from the literature, species composition was likely the leading factor affecting pDA concentrations in the GOM.

The presence of toxic *Pseudo-nitzschia* spp. is not the only factor for pDA concentrations, as production of DA can vary depending on life stage (Auro and Cochlan, 2013), light availability (Auro and Cochlan, 2013; Terseleer et al., 2013), macronutrients (Lema et al., 2017), nutrient ratios (Lema et al., 2017), trace metals (Wells et al., 2005), or even the presence/absence of predatory zooplankton (Lundholm et al., 2018; Tammilehto et al., 2015). The Wilcoxon signed-rank test indicated that Si:N of positive DA samples was significantly lower in 2016 than in 2012 and 2015, and that N:P was significantly higher in 2016 than in 2012 or 2015. This may be the result of the significantly higher ammonium concentrations that were measured in 2016, because, in the ratios, N was the sum of NO_x^- and NH^{4+}. However, Si* was also significantly lower in 2016, and that measurement is only a comparison between $Si(OH)_4$ and NO_x^-. Several lab studies have found DA production to increase under silicic acid-limiting conditions when nitrogen was abundant (Lema et al., 2017; Tatters et al., 2012; Terseleer et al., 2013). One field study also observed that maximum pDA concentrations occurred when both silicate and phosphate were limiting (Thorel et al., 2017). Although this ratio was not directly correlated with pDA concentrations in the present study, its role in triggering and enhancing DA production by *P. australis* and other species cannot be ignored.

Despite the laboratory evidence of the role of environmental factors

in DA production, it is difficult to translate lab results to the field. Communities in the lab are often monospecific, and all other factors besides the parameter in question are carefully controlled. In the field, there are typically many *Pseudo-nitzschia* species present as well as other plankton that interact with *Pseudo-nitzschia* and utilize nutrients. For example, grazer interactions have recently been shown to dramatically enhance DA production in *Pseudo-nitzschia* (Lundholm et al., 2018). As in this study, studies along the Washington and California coasts were unable to attribute DA concentrations or species abundance to a single environmental parameter (Smith et al., 2017; Trainer et al., 2009). The lack of simple correlations between environmental factors and pDA does not indicate that environmental factors are unimportant, but rather that pDA concentrations in the field likely depend on a combination of many different factors.

4.4. The 2016 event

The DA event in 2016 was unique from previous years in three ways. First, *P. australis* was identified for the first time in the GOM (Bates et al., 2018). Second, the bloom occurred in September and October, whereas in previous years *Pseudo-nitzschia* cell concentrations peaked in the spring or summer (Figs. 3 and 4) and the bloom season had been assumed to end in fall. Third, the species assemblage during the 2016 bloom was not a mix of *P. delicatissima*, *P. seriata*, *P. plurisecta*, and *P. pungens*, but rather dominated by one species. *P. australis* was present in every sample, and in many samples its relative abundance was more than 50% by ARISA estimates.

4.4.1. What caused the abnormally high pDA levels in 2016?

The historic shellfish closures in the GOM in 2016 prompt the question: why was pDA so high? PDA values in 2016 were likely the result of high *P. australis* relative abundance in combination with limiting silicic acid concentrations, but, of these, *P. australis* was the leading order factor in high pDA levels.

P. australis is one of the most toxic *Pseudo-nitzschia* species, both in this dataset and in the literature (Section 4.3). The presence of *P. australis* alone might be enough to explain the high pDA levels in 2016, because cDA was significantly higher in 2016 despite similar total cell counts. However, significantly lower Si* co-occurred with the *P. australis* cells in 2016, and DA production has been linked to silica stress in both the laboratory (Doucette et al., 2008; Terseleer et al., 2013), and the field (Marchetti et al., 2004; Ryan et al., 2017). Low Si* may have enhanced DA production by *P. australis* cells to create higher pDA concentrations. Because 2014 had equally low Si* to 2016 but pDA concentrations in line with 2012, 2013, and 2015, and since *P. australis* was not present in 2014, *P. australis* was probably the leading factor for the high pDA concentrations in 2016.

4.4.2. Where did P. australis originate?

The first hypothesis for the origin of *P. australis* is that it was present in undetectable amounts prior to 2016 and grew in 2016 because of altered environmental conditions. This hypothesis cannot be ruled out, but it seems unlikely, because there is little evidence to suggest that there were sufficient changes to growth conditions to favor a *P. australis* bloom. Nutrient concentrations and ratios were not significantly different in 2016 compared to all prior years. Si* was significantly lower in 2016 compared to 2012 and 2015, but this is expected to stress *Pseudo-nitzschia* cells, not improve their growth (Terseleer et al., 2013). There is no evidence in the literature to suggest that *P. australis* growth in particular improves with low silicic acid, so it is unknown whether low Si* might have enhanced *P. australis* growth over other *Pseudo-nitzschia* species. NH_4^+ was significantly higher in 2016 compared to 2012 and 2015, and in Puget Sound *P. australis* and *P. seriata* relative abundance were found to correlate with NH_4^+ (Hubbard et al., 2014), but growth experiments have not found significantly improved *P. australis* growth when nitrogen was in the NH_4^+ form (Howard et al., 2007; Martin-

Jézéquel et al., 2015). As previously discussed, it is difficult to draw conclusions about the conditions preceding a bloom from survey data alone. Thus, the differences in nutrients in 2016 do not conclusively point to improved conditions for *P. australis* growth.

Salinity was significantly higher in 2016 than in three previous years, suggesting a possible factor in the emergence of *P. australis*. It is possible for salinity to favor *P. australis* growth, because *P. australis* has been shown to prefer a more limited range of salinity relative to other species (Ayache et al., 2018), but the 2016 cruise data are insufficient to fully explore correlations between *P. australis* and salinity. The greater salinity values in 2016 compared to those in previous years (Fig. 10) could be explained in a number of ways, some of which point to other explanations for the *P. australis* bloom. The 2016 cruise occurred later in the year than previous years, and salinity typically increases through the summer and fall in the GOM. Salinity during the 2016 cruise was only slightly higher than regional climatology for that time of year (Fig. 10). Relatively low river discharge in 2016 also may have led to greater than average salinities inshore (supplementary material).

The high salinity values may also indicate an anomalous water mass, which relates to a hypothesis that *P. australis* was introduced into the GOM in 2016. Inflows from the Scotian Shelf and Northeast Channel vary in strength interannually (Townsend et al., 2014), and may provide a potential pathway for introducing *P. australis* cells. In particular, climatology from NERACOOS station M in Jordan Basin showed a rapid increase in salinity and temperature values in summer 2016 at 250 m (Fig. 11) that may have been associated with anomalously warm/salty eddies propagating from the Grand Banks near Novia Scotia (Brickman et al., 2018) or with Gulf Stream Ring water (GSRW). Townsend et al. (2015) showed evidence of GSRW, or a mixture containing a significant fraction of GSRW, that had penetrated at intermediate and bottom depths into Jordan Basin in the interior GOM in the fall of 2013. They analyzed a time series of temperature and salinity at Buoy M in Jordan Basin, as augmented by *in situ* nitrate data collected at 100 m with a Satlantic optical nitrate sensor (Twardowski et al., 2015). Nitrate served as a third semiconservative water mass tracer to identify an intrusion of anomalously warm and salty, but low nitrate, GSRW. Unlike low-nitrate GSRW, an intrusion of Warm Slope Water with similar T/S properties would have exhibited elevated nitrate concentrations (typically 16–17 μM; Townsend et al., 2006), not the drop from 12 μM to 8 μM that was observed (Townsend et al., 2015).

Similarly timed signals were observed at buoy station M in Jordan Basin in 2016 and in the late summer and fall in 2017 and 2018. Deep waters (at 200 m and 250 m) during those events exhibited the warmest and saltiest values of the time series in Jordan Basin (2003 to present) and were accompanied by lowered nitrate concentrations (Townsend, unpubl.), characteristic of GSRW (Townsend et al., 2010). Warm Core Rings can encompass 1500 m in the vertical (Joyce, 1984) which suggests that the signals observed at 250 m in 2016 and 100 m in 2013 (Townsend et al., 2015) could both have been caused by GSRW.

From GOM hydrodynamics, bloom timing, and experiments in *Pseudo-nitzschia* physiology, it is plausible that the *P. australis* cells observed in the Bay of Fundy and near eastern Maine in 2016 were carried in with a GSRW intrusion. The intrusion was observed in Jordan Basin in July. Assuming an average current speed of 10 cm s^{-1}, it would have taken one to two months for this water to circulate the basin and transit to the Bay of Fundy, where elevated DA concentrations led to shellfishery closures in early September 2016. Therefore, there was more than enough time for the water mass to advect to the bloom region, where it would be mixed into the upper water column by strong tidal pumping in those areas. Notably, this would also require a departure from the climatological circulation pictured in Fig. 1, which is possible in the event of an anomalous water mass intrusion. Because the anomaly in Jordan Basin was observed at 250 m, any *Pseudo-nitzschia* cells associated with this water mass would have been deep in the water column, and a question remains whether the cells can survive at depth

for an extended period of time. In a recent experiment, *Pseudo-nitzschia* spp. cultures (species not specified) were able to survive more than 6 weeks of complete darkness and resume growth with no lasting effects (Fang and Sommer, 2017).

Continuous plankton recorder (CPR) data from offshore and from on the Scotian Shelf in 2016 were examined to look for offshore peaks in large *Pseudo-nitzschia* cell concentrations, but none were found (refer to supplementary material for plots of CPR data). This does not completely rule out the North Atlantic as a source, however, because the CPR data had coarse temporal resolution and samples were only taken from the surface, so sub-surface populations would not have been detected. The intrusion hypothesis can therefore be neither refuted nor confirmed, and remains a possibility.

4.4.3. Hydrodynamics as drivers of the 2016 bloom

The cumulative upwelling index (CUI) gave important clues to the timing of the 2016 *P. australis* bloom. Wind direction has been shown to influence alongshore transport in the GOM: in 2010, strong upwelling-favorable winds in combination with a weak dynamic height gradient led to weak alongshore flow, reducing the alongshore extent of an *A. catenella* bloom (McGillicuddy et al., 2011). In 2016 the CUI began at a minimum in May and rapidly climbed to outpace every other year except 2013 (Section 3.5). Upwelling-favorable winds in 2016 may have reduced alongshore transport and led to *Pseudo-nitzschia* retention in the Bay of Fundy, where DA in excess of 20 μg g^{-1} of shellfish tissue was recorded from September 16–30 (Canadian Food Inspection Agency).

A rapid switch from upwelling-favorable to downwelling-favorable winds occurred from September 23rd to 27th, potentially accelerating alongshore flow and cell transport (Franks and Anderson, 1992). Shellfish closure timing aligned with alongshore transport time: shellfisheries in Cobscook Bay on the Canadian border were closed on September 27th, 2016, and shellfisheries at Mt. Desert Island 95 km away were closed 3 days later, on September 30th, 2016 (Rappaport, 2016). In addition, there were recalls of mussels and mahogany quahogs harvested near Jonesport, ME between September 25 and 30 and clams harvested near Corea, ME between September 28 and 30. From NERACOOS buoy I, the average surface current speed in 2016 was 0.3 m s^{-1}. Assuming this average, it would take less than a day for alongshore currents to transport cells from the Bay of Fundy to Cobscook Bay, and about 4 days for them to transport cells to Mt. Desert Island. These timelines and calculations are estimates, but they suggest that the shift from upwelling-favorable to downwelling-favorable winds on September 23rd–27th was a factor in bloom timing on the coast of Maine.

5. Conclusion

This paper builds on the work of Fernandes et al. (2014) by analyzing the spatial and temporal patterns in *Pseudo-nitzschia* species composition in the GOM. ARISA was used to identify 11 species from ship survey and time series samples in 2012, 2013, 2014, 2015, and 2016. Pre-2016, observed *Pseudo-nitzschia* blooms followed consistent biogeography in the GOM, with *P. pluriseta* inshore and *P. seriata* and *P. delicatissima* offshore. In addition, pDA concentrations increased with cell concentrations, toxic species relative abundance, and as a result of inter-species variation in cellular DA quotas.

Spatial, seasonal, and interannual variability in species composition and absolute cell abundance may have been influenced by seasonal and interannual variations in upwelling winds, North Atlantic inflows, cumulative river discharge, and alongshore transport. The effects of these regional patterns may have been modified by local variations in temperature, salinity, nutrient concentrations, and nutrient ratios, but in contrast to several other studies (e.g., Kaczmarska et al., 2007), no significant correlations between individual species and environmental factors, individual species and pDA, or environmental factors and pDA

were found. Increased relative abundance of toxic species led to increased pDA, but DA concentrations were likely caused by a combination of species composition and environmental factors.

Of particular interest was the 2016 *P. australis* bloom. This was the first known observation of *P. australis* in the GOM, and it was the first time in GOM history that shellfisheries were closed because DA concentrations exceeded the regulatory limit (Bates et al., 2018). Particulate DA concentrations reached 37.5 μg L^{-1} in 2016, which is comparable in magnitude to DA that has been measured on the west coast of the U.S. during *Pseudo-nitzschia* blooms. The high pDA in 2016 is attributed to the presence of *P. australis* in combination with low Si*. The source of *P. australis* is still unclear; we hypothesize that the species was carried in on an anomalous water mass in 2016, but more investigation is needed to determine the origin of these toxic cells, as well as the extent to which they persist within the GOM. Continued monitoring is essential both to improve the understanding of *Pseudo-nitzschia* bloom dynamics in the GOM and for the protection of public health.

Appendix A. Supplementary data

Supplementary material related to this article can be found, in the online version, at doi:https://doi.org/10.1016/j.hal.2019.101656.

References

Anderson, C.R., Brzezinski, M.A., Washburn, L., Kudela, R., 2006. Circulation and environmental conditions during a toxigenic Pseudo-nitzschia australis bloom in the Santa Barbara Channel, California. Mar. Ecol. Prog. Ser. 327, 119–133.

Auro, M.E., Cochlan, W.P., 2013. Nitrogen utilization and toxin production by two diatoms of the Pseudo-nitzschia pseudodelicatissima complex: P. cuspidata and P. fryxelliana. J. Phycol. 49, 156–169. https://doi.org/10.1111/jpy.12033.

Ayache, N., Hervé, F., Martin-Jézéquel, V., Amzil, Z., Caruana, A.M.N., 2018. Influence of sudden salinity variation on the physiology and domoic acid production by two strains of Pseudo-nitzschia australis. J. Phycol. 33, 0–3. https://doi.org/10.1111/jpy.12801.

Bates, S.S., Bird, C.J., de Freitas, A.S.W., Foxall, R., Gilgan, M., Hanic, L.A., Johnson, G.R., McCulloch, A.W., Odense, P., Pocklington, R., Quilliam, M.A., Sim, P.G., Smith, J.C., Subba Rao, D.V., Todd, E.C.D., Walter, J.A., Wright, J.L.C., 1989. Pennate diatom nitzschia pungens as the primary source of domoic acid, a toxin in shellfish from Eastern Prince Edward Island, Canada. Can. J. Fish. Aquat. Sci. 46, 1203–1215. https://doi.org/10.4224/23000873.

Bates, S.S., Hubbard, K.A., Lundholm, N., Montresor, M., Leaw, C.P., 2018. Pseudo-nitzschia, Nitzschia, and domoic acid: new research since 2011. Harmful Algae 79, 3–43. https://doi.org/10.1016/j.hal.2018.06.001.

Bisagni, J.J., Gifford, D.J., Ruhsam, C.M., 1996. The spatial and temporal distribution of

the Maine Coastal Current during 1982. Cont. Shelf Res. 16, 1–24.

Bowers, H.A., Ryan, J.P., Hayashi, K., Woods, A.L., Marin, R., Smith, G.J., Hubbard, K.A., Doucette, G.J., Mikulski, C.M., Gellene, A.G., Zhang, Y., Kudela, R.M., Caron, D.A., Birch, J.M., Scholin, C.A., 2018. Diversity and toxicity of Pseudo-nitzschia species in Monterey Bay: perspectives from targeted and adaptive sampling. Harmful Algae 78, 129–141. https://doi.org/10.1016/j.hal.2018.08.006.

Bresnan, E., Kraberg, A., Fraser, S., Brown, L., Hughes, S., Wiltshire, K.H., 2015. Diversity and seasonality of Pseudo-nitzschia (Peragallo) at two North Sea time-series monitoring sites. Helgol. Mar. Res. 69, 193–204. https://doi.org/10.1007/s10152-015-0428-5.

Brickman, D., Hebert, D., Wang, Z., 2018. Mechanism for the recent ocean warming events on the Scotian Shelf of eastern Canada. Cont. Shelf Res. 156, 11–22. https://doi.org/10.1016/j.csr.2018.01.001.

Canada, E., 2018. Water Level and Flow [WWW Document].

Cusack, C., Mouriño, H., Moita, M.T., Silke, J., 2015. Modelling Pseudo-nitzschia events off southwest Ireland. J. Sea Res. 105, 30–41. https://doi.org/10.1016/j.seares.2015.06.012.

Doucette, G.J., King, K.L., Thessen, A.E., Dortch, Q., 2008. The effect of salinity on domoic acid production by the diatom Pseudo-nitzschia multiseries. Nov. Hedwigia 133, 31–46.

Downes-Tettmar, N., Rowland, S., Widdicombe, C., Woodward, M., Llewellyn, C., 2013. Seasonal variation in Pseudo-nitzschia spp. and domoic acid in the Western English Channel. Cont. Shelf Res. 53, 40–49. https://doi.org/10.1016/j.csr.2012.10.011.

Fang, X., Sommer, U., 2017. Overwintering effects on the spring bloom dynamics of phytoplankton. J. Plankton Res. 39, 772–780. https://doi.org/10.1093/plankt/fbx046.

Fehling, J., Davidson, K., Bolch, C., Tett, P., 2006. Seasonality of Pseudo-nitzschia spp. (Bacillariophyceae) in western Scottish waters. Mar. Ecol. Prog. Ser. 323, 91–105.

Fehling, J., Green, D.H., Davidson, K., Botch, C.J., Bates, S.S., 2004. Domoic acid production by Pseudo-nitzschia seriata (bacillariophyceae) in Scottish waters. J. Phycol. 40, 622–630. https://doi.org/10.1111/j.1529-8817.2004.03200.x.

Fernandes, L.F., Hubbard, K.A., Richlen, M.L., Smith, J., Bates, S.S., Ehrman, J., Léger, C., Mafra, L.L., Kulis, D., Quilliam, M., Libera, K., McCauley, L., Anderson, D.M., 2014. Diversity and toxicity of the diatom Pseudo-nitzschia peragallo in the Gulf of Maine, Northwestern Atlantic Ocean. Deep. Res. Part II Top. Stud. Oceanogr. 103, 139–162. https://doi.org/10.1016/j.dsr2.2013.06.022.

Franks, P.J.S., Anderson, D.M., 1992. Marine Biology in a buoyancy current: Alexandrium tamarense in the Gulf of Maine. Mar. Biol. 112, 153–164.

Guannel, M.L., Haring, D., Twiner, M.J., Wang, Z., Noble, A.E., Lee, P.A., Saito, M.A., Rocap, G., 2015. Toxigenicity and biogeography of the diatom Pseudo-nitzschia across distinct environmental regimes in the South Atlantic Ocean. Mar. Ecol. Prog. Ser. 526, 67–87. https://doi.org/10.3354/meps11027.

Hansen, L.R., Soylu, S.í, Kotaki, Y., Moestrup, Ø., Lundholm, N., 2011. Toxin production and temperature-induced morphological variation of the diatom Pseudo-nitzschia seriata from the Arctic. Harmful Algae 10, 689–696. https://doi.org/10.1016/j.hal.2011.05.004.

Hasle, G.R., 2002. Are most of the domoic acid-producing species of the diatom genus Pseudo-nitzschia cosmopolites? Harmful Algae 1, 137–146. https://doi.org/10.1016/S1568-9883(02)00014-8.

Howard, M.D.A., Cochlan, W.P., Ladizinsky, N., Kudela, R.M., 2007. Nitrogenous preference of toxigenic Pseudo-nitzschia australis (Bacillariophyceae) from field and laboratory experiments. Harmful Algae 6, 206–217. https://doi.org/10.1016/j.hal.2006.06.003.

Hubbard, K.A., Olson, C.E., Armbrust, E.V., 2014. Molecular characterization of Pseudo-nitzschia community structure and species ecology in a hydrographically complex estuarine system (Puget Sound, Washington, USA). Mar. Ecol. Prog. Ser. 507, 39–55. https://doi.org/10.3354/meps10820.

Joyce, T., 1984. Velocity and hydrographic structure of a gulf stream warm-core ring. J. Phys. Oceanogr. 14, 936–947.

Keafer, B.A., Churchill, J.H., McGillicuddy, D.J., Anderson, D.M., 2005. Bloom development and transport of toxic Alexandrium fundyense populations within a coastal plume in the Gulf of Maine. Deep. Res. Part II Top. Stud. Oceanogr. 52, 2674–2697. https://doi.org/10.1016/j.dsr2.2005.06.016.

Large, W.G., Pond, S., 1981. Open ocean momentum flux measurements in moderate to strong winds. J. Phys. Oceanogr. https://doi.org/10.1175/1520-0485(1981)011<0324:OOMFMI>2.0.CO;2.

Lema, K.A., Latimier, M., Nézan, É., Fauchot, J., Le Gac, M., 2017. Inter and intra-specific growth and domoic acid production in relation to nutrient ratios and concentrations in Pseudo-nitzschia: phosphate an important factor. Harmful Algae 64, 11–19. https://doi.org/10.1016/j.hal.2017.03.001.

Li, Y., He, R., 2014. Spatial and temporal variability of SST and ocean color in the Gulf of Maine based on cloud-free SST and chlorophyll reconstructions in 2003-2012. Remote Sens. Environ. 144, 98–108. https://doi.org/10.1016/j.rse.2014.01.019.

Li, Y., He, R., McGillicuddy, D.J., 2014. Seasonal and interannual variability in Gulf of Maine hydrodynamics: 2002-2011. Deep. Res. Part II Top. Stud. Oceanogr. 103, 210–222. https://doi.org/10.1016/j.dsr2.2013.03.001.

Li, Y., He, R., McGillicuddy, D.J., Anderson, D.M., Keafer, B.A., 2009. Investigation of the 2006 Alexandrium fundyense bloom in the Gulf of Maine: in-situ observations and numerical modeling. Cont. Shelf Res. 29, 2069–2082. https://doi.org/10.1016/j.csr.2009.07.012.

Lundholm, N., Clarke, A., Ellegaard, M., 2010. A 100-year record of changing Pseudo-nitzschia species in a sill-fjord in Denmark related to nitrogen loading and temperature. Harmful Algae 9, 449–457. https://doi.org/10.1016/j.hal.2010.03.001.

Lundholm, N., Krock, B., John, U., Skov, J., Cheng, J., Pančić, M., Wohlrab, S., Rigby, K., Nielsen, T.G., Selander, E., Harðardóttir, S., 2018. Induction of domoic acid production in diatoms—types of grazers and diatoms are important. Harmful Algae.

https://doi.org/10.1016/j.hal.2018.06.005.

Lynch, D.R., Naimie, C.E., 1993. Tide and its residual on the outer banks of the Gulf of Maine. J. Phys. Oceanogr. https://doi.org/10.1175/1520-0485(1993)023<2222:TMTAIR>2.0.CO;2.

MacFadyen, A., Hickey, B.M., Foreman, M.G.G., 2005. Transport of surface waters from the Juan de Fuca eddy region to the Washington coast. Cont. Shelf Res. 25, 2008–2021. https://doi.org/10.1016/j.csr.2005.07.005.

Marchetti, A., Trainer, V.L., Harrison, P.J., 2004. Environmental conditions and phytoplankton dynamics associated with Pseudo-nitzschia abundance and domoic acid in the Juan de Fuca eddy. Mar. Ecol. Prog. Ser. 281, 1–12. https://doi.org/10.3354/meps281001.

Martin-Jézéquel, V., Calu, G., Candela, L., Amzil, Z., Jauffrais, T., Séchet, V., Weigel, P., 2015. Effects of organic and inorganic nitrogen on the growth and production of domoic acid by Pseudo-nitzschia multiseries and P. australis (bacillariophyceae) in culture. Mar. Drugs 13, 7067–7086. https://doi.org/10.3390/md13127055.

McCabe, R.M., Hickey, B.M., Kudela, R.M., Lefebvre, K.A., Adams, N.G., Bill, B.D., Gulland, F.M.D., Thomson, R.E., Cochlan, W.P., Trainer, V.L., 2016. An unprecedented coastwide toxic algal bloom linked to anomalous ocean conditions. Geophys. Res. Lett. 43, 10,366–10,376. https://doi.org/10.1002/2016GL070023.

McGillicuddy, D.J., Townsend, D.W., He, R., Keafer, Ba, Kleindinst, J.L., Li, Y., Manning, J.P., Mountain, D.G., Thomas, Ma, Anderson, D.M., 2011. Suppression of the 2010 Alexandrium fundyense bloom by changes in physical, biological, and chemical properties of the Gulf of Maine. Limnol. Oceanogr. 56, 2411–2426. https://doi.org/10.4319/lo.2011.56.6.2411.

Morrison, J.R., 2019. No Title [WWW Document]. Northeast. Reg. Assoc. Coast. Ocean Obs. Syst. URL. http://neracoos.org/.

Palma, S., Mouriño, H., Silva, A., Barão, M.I., Moita, M.T., 2010. Can Pseudo-nitzschia blooms be modeled by coastal upwelling in Lisbon Bay? Harmful Algae 9, 294–303. https://doi.org/10.1016/j.hal.2009.11.006.

Parsons, M.L., Dortch, Q., Turner, R.E., 2002. Sedimentological evidence of an increase in Pseudo-nitzschia (Bacillariophyceae) abundance in response to coastal eutrophication. Limnol. Oceanogr. 47, 551–558. https://doi.org/10.4319/lo.2002.47.2.0551.

Pettigrew, N.R., Churchill, J.H., Janzen, C.D., Mangum, L.J., Signell, R.P., Thomas, A.C., Townsend, D.W., Wallinga, J.P., Xue, H., 2005. The kinematic and hydrographic structure of the Gulf of Maine Coastal Current. Deep. Res. Part II Top. Stud. Oceanogr. 52, 2369–2391. https://doi.org/10.1016/j.dsr2.2005.06.033.

Quijano-Scheggia, S., Garcés, E., Flo, E., Fernández-Tejedor, M., Diogène, J., Camp, J., 2008. Bloom dynamics of the genus Pseudo-nitzschia (Bacillariophyceae) in two coastal bays (NW Mediterranean Sea). Sci. Mar. 72, 577–590. https://doi.org/10.3989/scimar.2008.72n3577.

Rappaport, S., 2016. Shellfish Closure Expanded; Cost to Industry Mounts. Ellsworth Am.

Ryan, J.P., Kudela, R.M., Birch, J.M., Blum, M., Bowers, H.A., Chavez, F.P., Doucette, G.J., Hayashi, K., Marin, R., Mikulski, C.M., Pennington, J.T., Scholin, C.A., Smith, G.J., Woods, A., Zhang, Y., 2017. Causality of an extreme harmful algal bloom in Monterey Bay, California, during the 2014–2016 northeast Pacific warm anomaly. Geophys. Res. Lett. 44, 5571–5579. https://doi.org/10.1002/2017GL072637.

Santiago-Morales, I.S., García-Mendoza, E., 2011. Growth and domoic acid content of Pseudo-nitzschia australis isolated from northwestern Baja California, Mexico, cultured under batch conditions at different temperatures and two Si:NO3 ratios. Harmful Algae 12, 82–94. https://doi.org/10.1016/j.hal.2011.09.004.

Schnetzer, A., Jones, B.H., Schaffner, R.A., Cetinic, I., Fitzpatrick, E., Miller, P.E., Seubert, E.L., Caron, D.A., 2013. Coastal upwelling linked to toxic Pseudo-nitzschia australis blooms in Los Angeles coastal waters, 2005-2007. J. Plankton Res. 35, 1080–1092. https://doi.org/10.1093/plankt/fbt051.

Schwing, F.B., O'Farrel, M., Steger, J.M., Baltz, K., 1996. Coastal Upwelling Indices, West Coast of North America, 1946-1995. NOAA Tech. Memo. NMFS-SWFSC-231 671. pp. 1–45.

Sekula-Wood, E., Benitez-Nelson, C., Morton, S., Anderson, C., Burrell, C., Thunell, R., 2011. Pseudo-nitzschia and domoic acid fluxes in Santa Barbara Basin (CA) from 1993 to 2008. Harmful Algae 10, 567–575. https://doi.org/10.1016/J.HAL.2011.04.009.

Smith, J., Gellene, A.G., Hubbard, K.A., Bowers, H.A., Kudela, R.M., Hayashi, K., Caron, D.A., 2017. Pseudo-nitzschia species composition varies concurrently with domoic acid concentrations during two different bloom events in the Southern California Bight. J. Plankton Res. 40, 1–17. https://doi.org/10.1093/plankt/fbx069.

Tammilehto, A., Nielsen, T.G., Krock, B., Møller, E.F., Lundholm, N., 2015. Induction of domoic acid production in the toxic diatom Pseudo-nitzschia seriata by calanoid copepods. Aquat. Toxicol. 159, 52–61. https://doi.org/10.1016/j.aquatox.2014.11.026.

Tatters, A.O., Fu, F.X., Hutchins, D.A., 2012. High CO 2 and silicate limitation synergistically increase the toxicity of Pseudo-nitzschia fraudulenta. PLoS One 7. https://doi.org/10.1371/journal.pone.0032116.

Terseleer, N., Gypens, N., Lancelot, C., 2013. Factors controlling the production of domoic acid by Pseudo-nitzschia (Bacillariophyceae): a model study. Harmful Algae 24, 45–53. https://doi.org/10.1016/j.hal.2013.01.004.

Thessen, A.E., Stoecker, D.K., 2008. Distribution, abundance and domoic acid analysis of the toxic diatom genus Pseudo-nitzschia from the Chesapeake Bay. Estuaries Coasts 31, 664–672. https://doi.org/10.1007/s12237-008-9053-8.

Thorel, M., Claquin, P., Schapira, M., Le Gendre, R., Riou, P., Goux, D., Le Roy, B., Raimbault, V., Deton-Cabanillas, A.F., Bazin, P., Kientz-Bouchart, V., Fauchot, J., 2017. Nutrient ratios influence variability in Pseudo-nitzschia species diversity and particulate domoic acid production in the Bay of Seine (France). Harmful Algae 68, 192–205. https://doi.org/10.1016/j.hal.2017.07.005.

Townsend, D.W., McGillicuddy, D.J., Thomas, M.A., Rebuck, N.D., 2014. Nutrients and water masses in the Gulf of Maine-Georges Bank region: variability and importance to blooms of the toxic dinoflagellate Alexandrium fundyense. Deep. Res. Part II Top.

Stud. Oceanogr. 103, 238–263. https://doi.org/10.1016/j.dsr2.2013.08.003.

Townsend, D.W., Pettigrew, N.R., Thomas, M.A., Neary, M.G., Mcgillicuddy, D.J., Donnell, J.O., 2015. Water masses and nutrient sources to the Gulf of Maine. J. Mar. Res. 141, 93–122. https://doi.org/10.1038/141548c0.

Townsend, D.W., Rebuck, N.D., Thomas, M.A., Karp-Boss, L., Gettings, R.M., 2010. A changing nutrient regime in the Gulf of Maine. Cont. Shelf Res. 30, 820–832. https://doi.org/10.1016/j.csr.2010.01.019.

Townsend, D.W., Thomas, A.C., Mayer, L.M., Thomas, M.A., Quinlan, J.A., 2006. Oceanography of the Northwest Atlantic shelf (1, W). The Sea: The Global Coastal Ocean: Interdisciplinary Regional Studies and Syntheses. Harvard University Press, pp. 119–168.

Trainer, V.L., Bates, S.S., Lundholm, N., Thessen, A.E., Cochlan, W.P., Adams, N.G., Trick, C.G., 2012. Pseudo-nitzschia physiological ecology, phylogeny, toxicity, monitoring and impacts on ecosystem health. Harmful Algae 14, 271–300. https://doi.org/10.1016/j.hal.2011.10.025.

Trainer, V.L., Hickey, B.M., Horner, R.A., 2002. Biological and physical dynamics of domoic acid production off the Washington coast. Limnol. Oceanogr. 47, 1438–1446. https://doi.org/10.4319/lo.2002.47.5.1438.

Trainer, V.L., Hickey, B.M., Lessard, E.J., Cochlan, W.P., Trick, C.G., Wells, M.L., MacFadyen, A., Moore, S.K., 2009. Variability of Pseudo-nitzschia and domoic acid in the Juan de Fuca eddy region and its adjacent shelves. Limnol. Oceanogr. 54, 289–308. https://doi.org/10.4319/lo.2009.54.1.0289.

Twardowski, M.S., Townsend, D.W., Sullivan, J.M., Koch, C., Pettigrew, N.R., O'Donnell, J., Stymiest, C., Salisbury, J., Moore, T., Young-Morse, R., Stockley, N.D., Morrison, J.R., 2015. Developing the first operational nutrient observatory for ecosystem, climate, and hazard monitoring for NERACOOS. Mar. Technol. Soc. J. 49, 72–80. https://doi.org/10.4031/MTSJ.49.3.11.

USGS, 2013. Water Data for the Nation [WWW Document]. URL. https://waterdata.usgs.gov/nwis.

Wang, Z., King, K.L., Ramsdell, J.S., Doucette, G.J., 2007. Determination of domoic acid in seawater and phytoplankton by liquid chromatography-tandem mass spectrometry. J. Chromatogr. A 1163, 169–176. https://doi.org/10.1016/j.chroma.2007.06.054.

Wells, M.L., Trick, C.G., Cochlan, W.P., Hughes, M.P., Trainer, V.L., 2005. Domoic acid: the synergy of iron, copper, and the toxicity of diatoms. Limnol. Oceanogr. 50 (6), 1908–1917.

Xue, H., Chai, F., Pettigrew, N.R., 2000. A model study of the seasonal circulation in the Gulf of Maine. J. Phys. Oceanogr. 30, 1111–1135. https://doi.org/10.1175/1520-0485(2000)030<1111:AMSOTS>2.0.CO;2.